33rd Annual International Conference of the IEEE EMBS
Boston, Massachusetts USA, August 30 - September 3, 2011

Development of Three Dimensional Blood Vessel Search System by Using on Stereo and Autofocus Hybrid Method

E. Nakamachi, *Member, IEEE*

Abstract— **In this study, we developed an accurate three dimensional blood vessel search (3D BVS) system and an automatic operated blood sampling system. These systems were implemented into the point-of-care system for the ubiquitous medical care, which was featured as the portable type self-monitoring blood glucose (SMBG) devise. It resolved the human error problem, which causes by the complicated manual operation of blood sampling and blood glucose measurement in conventional SMBG devices. In this study, we mainly discuss the performance examination of accurate position detection of blood vessel. Our 3D BVS system employed the near-infrared (NIR) light imaging process and the stereo and autofocus hybrid method to determine the 3D blood vessel location accurately. We evaluated the accuracy of our 3D BVS system by using the phantom of human skin, blood vessel and blood. As a result, we validated a very good performance ability of our 3D BVS system for a portable type SMBG device**

I. Introduction

Recently, the number of diabetic patients has increased rapidly, and it is becoming a major serious social problem [1]. So, it will be more important for our lives than ever to measure the blood glucose for self monitoring blood glucose (SMBG) system as a daily medical care for diabetic patients and its candidates. There are still a lot of improvement requirements in SMBG devices for high accurate and easy blood sampling and blood glucose measurement [2]-[10]. Nakamachi et al. have developed the three dimensional blood vessel search (3D BVS) system by using the NIR light [11]. However, its accuracy of blood position detection was still not enough.

In this study, I set my goal to develop a new comprehensive three dimensional blood vessel search (3D BVS) system device for automatically operated blood sampling and blood glucose measurement. At first, we employ the stereo and autofocus hybrid method for three dimensional blood vessel search (3D BVS) by using NIR light and image processing technique. Next, we evaluate the accuracy of 3D BVS system. Finally we examine automatic blood sampling and blood glucose measurement.

II. 3D Blood Vessel Position Search System

We detect three dimensional position of blood vessel for blood sampling. Our previous studies could not determine the depths of the vessels accurately. The measurement error

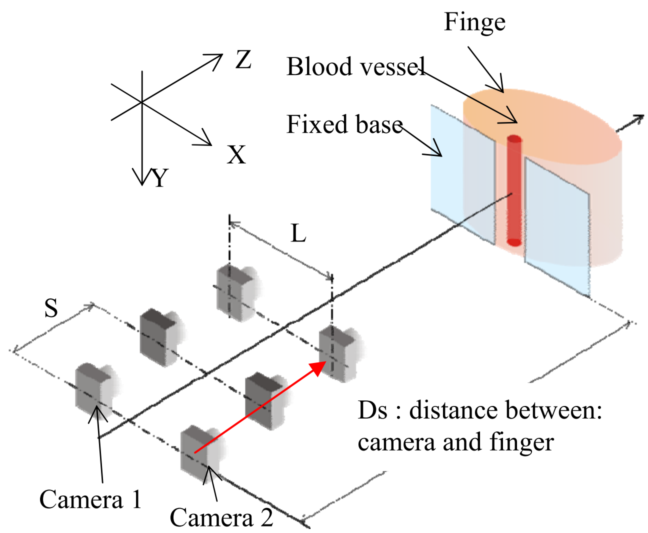

(a) Various positions of camera in autofocus method

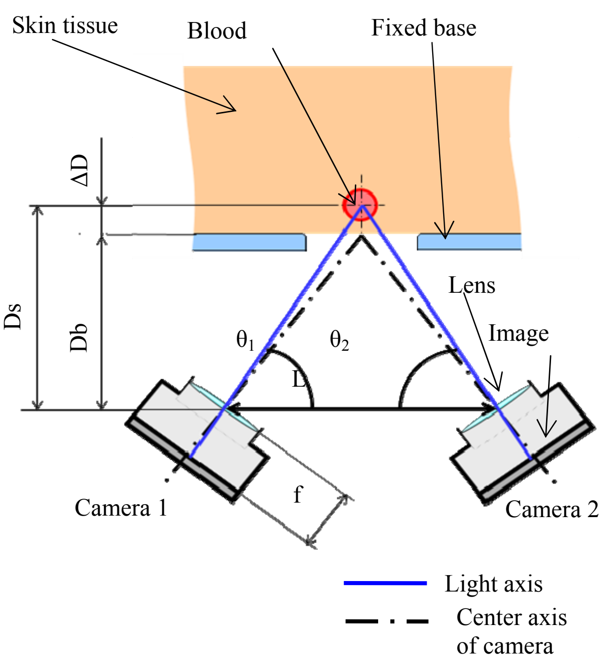

(b) Schematic view of the stereo optical system embedded in 3D BVS system

Fig. 1 Schematic diagram of the autofocus and stereo hybrid system embedded in 3D BVS system.

Manuscript received March 24, 2011, E. Nakamachi is with Doshisha University, Dept. of Biomedical Engng., 1-3 Miyakodani Tatara, Kyotanabe, Kyoto, 610-0394, Japan (e-mail: enakamac@mail.doshisha.ac.jp).

increased more as the depth of blood vessel in the finger increased. Therefore, we adopt stereo and autofocus hybrid method to detect the position of blood vessel with very high accuracy by obtaining the clear image. I adopted NIR light which had wavelengths between 700 nm and 1000 nm. We examined repeatedly and finally determined that a wavelength 870 nm had a most clear blood vessel image in the finger [11]. As shown in Fig. 1(a), we took blood vessel images by moving camera position towards the finger in the autofocus method. We evaluate the sharpness of the blood vessel image by the template matching algorithm and select a most clear image [11]. Next, we measured blood vessel position using the stereo method as shown Figure 1(b) [12], in which *L* is the length between two CMOS cameras, *F* the focal length, *Db* the vertical distance between the center of the blood vessel and the line drawn between two center points of the lenses, *Ds* the vertical distance between the reference surface of the fixed base and the line drawn between two center points of the lenses. ΔD is the depth of the blood vessel center from the reference surface. θ_1 and θ_2 are angles of the light axes from the center of the blood vessel against the horizontal line between the centers of two lenses as shown in Fig.3. The center of the blood vessel can be detected from the luminance distribution of the blood vessel images obtained by two cameras. θ_1 and θ_2 can be calculated by using trigonometric functions. *Db* is expressed as follow.

$$D_b = \frac{\tan\theta_1 \cdot \tan\theta_2}{\tan\theta_1 + \tan\theta_2} L \qquad (1)$$

The length *Ds* is a known value, so the depth of the blood vessel (ΔD) can be calculated as follow.

$$\Delta D = D_b - D_s \qquad (2)$$

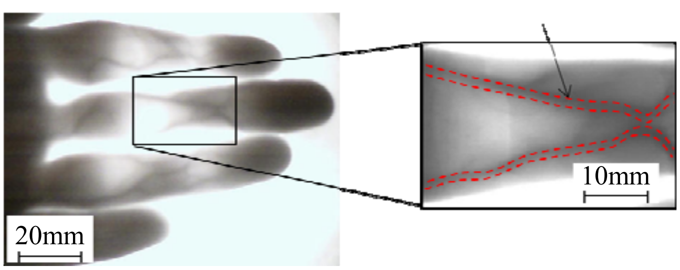

Fig. 2 Image of human blood vessel in the finger, where the wavelength of NIR light is 870 nm.

Fig.2 shows the image of finger and its enlarged image to confirm the blood vessel. Fig. 3 shows a prototype of BVS system. We assembled 3D BVS system by using four NIR LED (KYOSEMI, KED871M51A, peak wavelength 870 nm) for the light source, two CMOS cameras (ASAHI DENSHI, PPV404C) and two image processing units (ASAHI DENSHI, PP-DEB-007). The NIR LED was set behind the finger and irradiated against the finger. Two CMOS cameras took images of the blood vessel and calculate the position of blood vessel. Camera's focal length is 5.32 mm, its size is 8 × 8 × 5.55 mm and its image has 640 × 480 pixels in the rectangular image receiving plane. The pixel size is 3.6 × 3.6 μm. The pixel has 8bit digital gray scale value (black: 0 ~ white: 255) and those data was stored in Jpeg image file. The image processing unit (ASAHI DENSHI, AT401) was used to capture two images and calculate the depth of blood vessel from the finger surface.

Table 1 shows the specification of NIR light and CMOS camera.

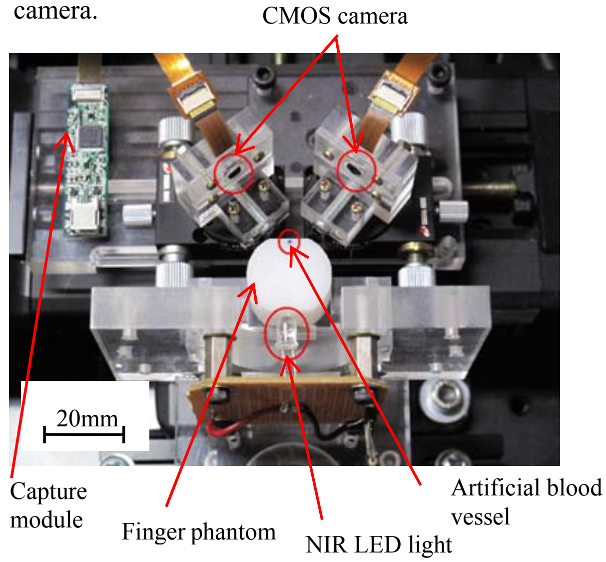

Fig.3 Prototype of 3D blood vessel searching system

Table 1 Specifications of NIR light and CMOS camera

NIR LED Light	Peak wavelength	871 (nm)
	Spectral bandwidth at 50%	40nm
	Peak emission wavelength	870 (nm)
	Half angle	15 (degree)
	Optical output power	18 (mW)
CMOS camera	Number of pixels	640×480 (pixel)
	Pixel size	3.6 (μm/pixel)
	Angle of camera inclination	38 (degree)
	Length between phantom and camera lens	Ds = 20 (mm)
	Length between right camera and left camera	L = 30 (mm)

III. EVALUATION OF BLOOD VESSEL SEARCH SYSTEM

We used the artificial finger phantom, in which the artificial blood vessels with colored liquid inside were embedded at the known depths ranged between 0.5mm and 2.5mm with 0.25mm interval. The finger phantom was made of polyacetal resin (Toyo Plastic Seiko CO., LTD., TPS-POM), which had the similar optical characteristics to the human skin [14]. Figure 4(a) shows the images of the artificial blood vessels at 1.0mm depth taken by two cameras.

The luminance data on the lines colored by blue and red at the middle in Y direction as shown in Fig. 4(a), such as the raw of pixel data from (X, Y) = (0, 240) to (640, 240), were used to calculate the depth by employing equations (1)-(2). We used the position data at the bottoms of luminance curves as shown in Fig. 4(b). We obtained depths of eight cases and found the errors caused by the refraction and scattering of NIR light. At first, we increased the electric power of NIR light to have higher penetration energy and succeeded to decrease the scattering and got very clear images with 50mW power. Next, NIR light was refracted at the interface between the air and the finger phantom, since the refractive index of polyacetal differs that of air. So the difference between the blood vessel position on the image and real one occurred. Therefore, we corrected the result of the measurements using Snell's law and the refractive index of the polyacetal as 1.48. Figure 5 shows the trajectory of NIR light from the finger phantom to the camera. It shows that the measured depth of the blood vessel become smaller than the real depths due to the refraction of NIR light. These are the formula for the incidence angle, refracting angle, and the blood vessel depth on the image in equations (3) - (5). Consequently, we had a maximum standard deviation as 111μm and an average of the standard deviation as 63μm. A good correlation ($R^2 = 0.946$) between the calculated depths and real depths was obtained as shown in Fig. 6. These errors are less than allowance value of 150 μm for the target of blood vessel, which diameter is more than 500 μm. We concluded that our 3D BVS system had a enough performance ability to detect the blood vessel position for automatically operated blood sampling.

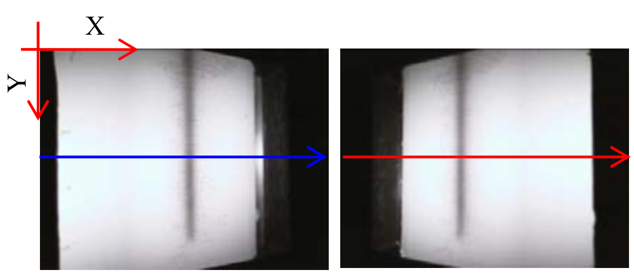

Camera 1 Camera 2

(a) Stereo images of the blood vessel

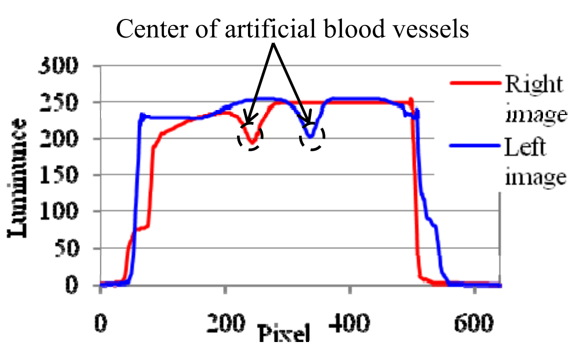

(b) Luminance distributions pixels in the central

Fig. 4 Example of images and luminance distributions

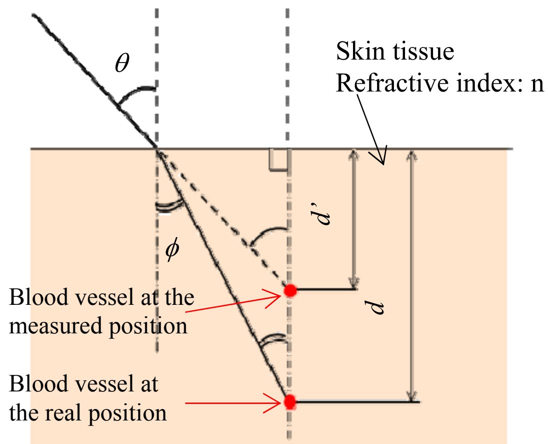

θ: Refraction angle
ϕ: Incidence angle
f: Focus length
s: Disparity of image
n: Refractive index
d: Real depth
d': Measured depth

$$\theta = \sin^{-1}\left(\frac{\sin\theta}{n}\right) \quad (3)$$

$$\phi = \tan^{-1}\left(\frac{f}{s}\right) \quad (4)$$

$$d = d'\frac{\tan\theta}{\tan\phi} \quad (5)$$

Fig. 5 Refraction of light in the skin tissue

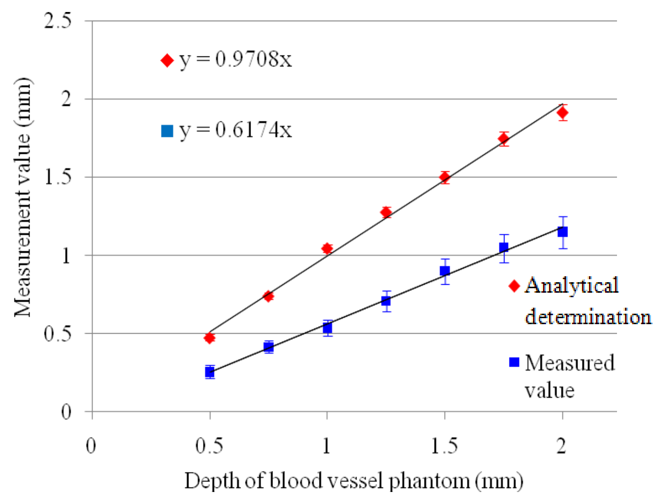

Fig. 6 Relationship between measured depth and assigned depth of artificial blood vessel.

IV. AUTOMATICALLY OPERATED BLOOD SAMPLING AND BLOOD GLUCOSE MEASUREMENT SYSTEM

We developed an automatically operated blood sampling system with blood glucose measurement system for a portable type SMBG device. In the previous study, an incomplete blood sampling system was embedded into the blood glucose measurement system [13], where HORIBA Ltd. made glucose enzyme sensor was used. We utilized two stepping-motors and two liner sliders for blood sampling and transportation. Figure 7(a) shows the photo of our SMBG system. The artificial finger was made of silicon rubber (Asahi Chemical Industries, Ltd., RTV2 VP7550) which has similar viscoelastic property of human skin. The diameter of an artificial blood vessel was 1.0 mm and the depth 1.0mm. We used

50% glycerin solution as the artificial blood which has a similar viscosity to the human blood. Fig. 7(b) shows the automatically operated blood sampling and transporting unit. After trial and error, we determined the piston speed as 1.0 mm/s to provide 5.0 µl artificial blood on the glucose enzyme sensor as shown in Fig. 7(c).

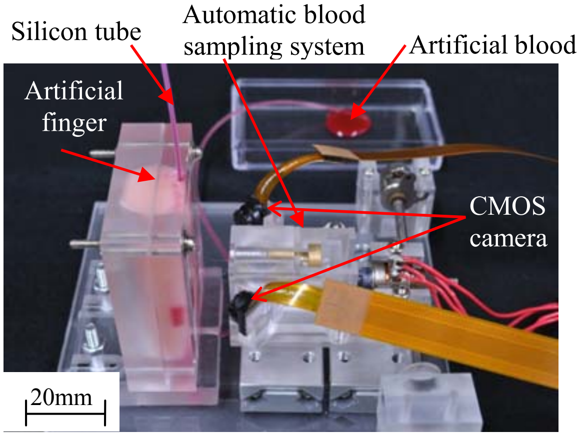

(a) Overview of SMBG system

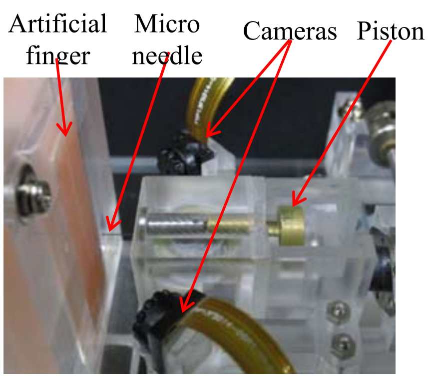

(b) Blood sampling and transportation unit

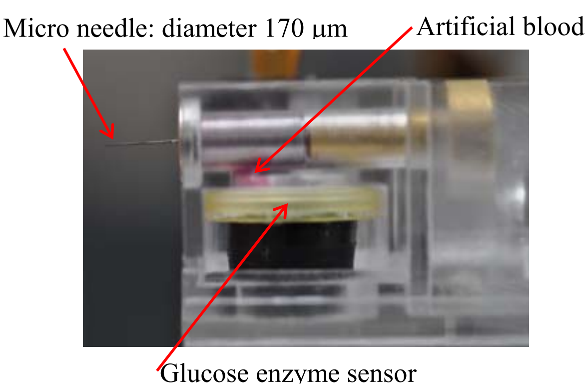

(c) Blood glucose sensor

Fig. 7 3D BVS, automatically operated blood sampling and blood glucose measurement units.

V. CONCLUSION

Results are summarized as follows: (1) Accuracy evaluation of 3D BVS system: a maximum standard deviation was 111µm and an average of the standard deviation was 63µm to detect 0.5mm diameter blood vessel embedded at depths ranged from 0.5mm to 2.5mm with 0.25mm interval. Consequently, we obtained the best correlation factor, R^2 = 0.946. (2) SMBG performance evaluation: the piston speed for blood suction and discharge was selected as 1.0 mm/s to provide 0.5µl artificial blood on the glucose enzyme sensor. It was enough amount to measure the blood glucose amount.

REFERENCES

[1] Matsushita Co. Ltd, "Blood sugar level measurement system (in Japanese)," Matsushita Technical Journal, 51(3), 2005, pp. 248-253.

[2] M. Miyazaki, "Reliability related to small size and simple blood sugar weighing device and the usages (in Japanese)," Journal of Clinical Laboratory Instruments and Reagents, 28(4), 2005, pp. 291-304.

[3] N. Ozeki, Y. Kamata, Y. Okuzumi, M. Fujishiro, K. Kawamura, M. Shibazaki, N. Shimetani and M. Mori, "Examination concerning measurement accuracy of small electrode type blood sugar measuring instrument Antsense III (in Japanese)," Journal of Medicine and Pharmaceutical Science, 53(3), 2005, pp. 361-370.

[4] K. Jungheim and T. Koschinsky, "Risky delay of hypoglycemia detection by glucose monitoring at the arm," Diabetes Care, 24, 2004, pp. 1303-1304.

[5] K. Fujita, K. Tamura, K. Wataru, H. Ishizawa and E. Toba, "Development of Noninvasive Blood Glucose Sensor Using the Infrared Spectroscopy (in Japanese)," Trans.Inst. Elect.Engnr.Jpn. C, 129(9), 2004, pp. 1759-1765.

[6] T. Karatsu, T. Nakajima, S. Yagai, M. Seimiya, F. Nomura and A. Kitamura, "Determination of the Glucose in Serum by the FT-IR-ATR Method," Japan analyst, 54(2), 2005, pp. 149-154.

[7] E. Nakamachi, S. Jinnin, Y. Uetsuji, K. Tsuchiya and H. Yamamoto, "Sputter Generating and Characterization of a Titanium Alloy Microneedle for Applying to Bio-MEM," Transactions of the Japan Society of Mechanical Engineers. A, 72(716), 2006, pp. 471-477.

[8] T. Asakura, and H. Seino, "Basic Study on a Micro-tapered needle (TN-3305) Used for Insulin Pre-filled Products," Japanese journal of pharmaceutical health care and sciences, 30(6), 2004, pp. 368-376.

[9] H. A. Mackenzie, H. S. Ashton, S. Spiers, Y. Shen, S. S. Freeborn, J. Hannigan, J. Lindberg and P. Rae, "Advances in photoacoustic noninvasive glucose testing," Clinical Chemistry, 45, 1999, pp. 1587-1595.

[10] K. Yamakoshi, S. Ishimaru, A. Nakabayashi, A. Okamoto, M. Nogawa, M. Maruyama and S. Tanaka, "Development of a compact device for self-monitoring of venous blood glucose using miniature needle and infra-red CCD monitor (in Japanese)," Transactions of the Japanese Society for Medical and Biological Engineering, 42, 2003, p. 198.

[11] E. Nakamachi, T. Kuroda, K. Tsuchiya, T. Uenoya and Y. Uetsuji, "Development of a Three-Dimensional Blood Vessel Searching System by Using the Near Infra-Red Light," Transactions of the Japan Society of Mechanical Engineers. C, 73(731), 2007, pp. 2088-2094.

[12] N. Furuya, "3D Measuring System for Assembly Robot Using Stereo Camera. Camera Model and Parameter Calibration by Geometrical Method", Journal of the Japan Society for Precision Engineering," 65(8), 1999, pp. 1116-1120.

[13] E. Nakamachi, "Development of Automatic Operated Blood Sampling System for Portable Type Self-Monitoring Blood Glucose," Proc. of IEEE Engineering in Medicine and Biology Society, 2010, pp. 335 - 338.

[14] Furuya, N., "3D Measuring System for Assembly Robot Using Stereo Camera. Camera Model and Parameter Calibration by Geometrical Method", Journal of the Japan Society for Precision Engineering, 65(8), 1999, pp. 1116-1120.